Original Article

Old spontaneously hypertensive rats gather together typical features of human chronic left-ventricular dysfunction with preserved ejection fraction

Halim Marzak[a], Estelle Ayme-Dietrich[a], Roland Lawson[a], Walid Mokni[a], Roy Combe[b], Julien Becker[b], Lahcen El Fertak[b], Marie-France Champy[b], and Laurent Monassier[a,b]

Objective: Heart failure with preserved left-ventricular ejection fraction (HF-PEF) is an entity leading to pulmonary congestion because of impaired diastolic filling. This syndrome usually strikes those who have experienced a long history of hypertension or metabolic risk factors. Pathophysiological mechanisms are not fully understood, and standard therapy is not established. Relevant preclinical models are still lacking. The aim of this work was to evaluate aging spontaneously hypertensive rats (SHRs) as a model of HF-PEF.

Methods: Serial echocardiographic and blood pressure (BP) measurements were performed in 28, 36, 43, 47 and 51-week-old SHRs and their normotensive controls (Wistar–Kyoto rats). In 52–53-week-old animals, final investigations included ECG, invasive left-ventricular (LV) and aortic catheterization, brain natriuretic peptide (BNP) plasma concentrations, ventricular reverse transcription-qPCR evaluations (β-myosin heavy chain, atrial natriuretic peptide, BNP, sarco/endoplasmic reticulum calcium ATPase 2a and collagens 1a, 3a and 2a) and cardiac histology.

Results: SHRs develop a progressive alteration of the early diastole, some of the echocardiographic parameters being not sensitive to BP reduction by the calcium blocker, nicardipine. The systolic function evaluated by echocardiography and invasive catheterization was preserved. When the observation period was over, an increase in collagen synthesis and deposits were identified in subendocardial layers. This attested a probable myocardial ischemia that was confirmed by ECG changes of the ST segment. BNP increased in the blood and at the mRNA level in the myocardium.

Conclusion: When aging, SHRs progressively develop HF-PEF showed by impaired LV relaxation and hypertrophy, BNP increase but preserved contractility and fibrosis. This model seems pertinent for further pharmacological preclinical studies in the field.

Keywords: cardiac hypertrophy, diastole, ejection fraction, hypertension, ischemia, nicardipine, spontaneously hypertensive rat

Abbreviations: β-MHC, myosin heavy chain β; ANP, atrial natriuretic peptide; BNP, brain natriuretic peptide; BP, blood pressure; DAP, diastolic arterial pressure; EDLVD, left-ventricular end diastolic diameter; ESLVD, left-ventricular end systolic diameter; HF-PEF, heart failure with preserved ejection fraction; HR, heart rate; IVRT, isovolumetric relaxation time; LV, left-ventricle; LVSP, left-ventricular systolic pressure; LVW, left-ventricular weight; PW, posterior wall; SAP, systolic arterial pressure; SERCA, sarco/endoplasmic reticulum calcium ATPase; SF, shortening fraction; SHRs, spontaneously hypertensive rats; SW, septal wall; WKYs, Wistar–Kyoto rats

INTRODUCTION

Heart failure with preserved left-ventricular ejection fraction (HF-PEF) is characterized by symptoms and signs of heart failure in patients showing a left-ventricular (LV) diastolic dysfunction with an ejection fraction over 40–50% measured by echocardiography [1]. Nowadays, nearly half of the patients with heart failure exhibit an LV ejection fraction over this threshold [2,3]. Mainly observed in the elderly, this syndrome is usually associated with a long history of high blood pressure (BP). Mortality reported by different studies varies greatly. Nevertheless, annual mortality remains lower for patients with HF-PEF compared with those having systolic heart failure. To date, no treatment has demonstrated any significant improvement of the survival of patients with HF-PEF [4,5], and predictive preclinical experimental models are cruelly missing. Only sparse studies investigated rodents as models of HF-PEF [6]. Unfortunately, most of these studies were deficient in longitudinal follow-up and in-depth investigations. Moreover, most of them were using invasive technologies requiring anesthesia and procedures

Journal of Hypertension 2014, 32:1307–1316

[a]Laboratoire de Neurobiologie et Pharmacologie Cardiovasculaire, Faculté de Médecine, Fédération de Médecine translationnelle, Université et Centre Hospitalier de Strasbourg, Strasbourg and [b]Mouse Clinical Institute, Illkirch-Graffenstaden, France

Correspondence to Laurent Monassier, MD, PhD, Laboratoire de Neurobiologie et Pharmacologie Cardiovasculaire, Faculté de Médecine, 11 rue Humann, 67085, Strasbourg Cedex, France. Tel: +33368853392; fax: +33368853388; e-mail: laurent.monassier@unistra.fr

Received 30 September 2013 **Revised** 28 January 2014 **Accepted** 1 February 2014

DOI:10.1097/HJH.0000000000000159

far from human investigations. Echocardiography is now the reference clinical tool to assess cardiac anatomy and function. The recent standardization of techniques and methods provides a unique opportunity to simultaneously obtain accurate measurements of LV morphology, mass and geometry [7], and the recent development of Doppler techniques makes possible cardiac systolic and diastolic functions evaluation [8]. A few years ago, these methods were transferred to rodents, such as rats and mice. Spontaneously hypertensive rats (SHRs) have been widely used for experimental research. They demonstrate high BP and concentric LV hypertrophy. Systolic heart failure is observed only in very old animals, survival being not constantly modified. A long-term echocardiographic follow-up of the LV function in adult SHRs and in their normotensive counterparts [Wistar–Kyoto rats (WKYs)] has lately been published [9]. Unfortunately, no data were provided between 36 and 60 weeks old, and correlations with ECG and histological findings were not documented. Moreover, the link between alterations of echocardiographic parameters and their relation to high BP was not determined. Therefore, the present study aimed at following male SHRs between 28 and 53 weeks of age to longitudinally characterize LV function and morphology by sequential echocardiography in parallel with BP measurements. We determined the link between echocardiographic diastolic parameters and afterload. At the end of the study, cardiac remodeling at histological, ECG and molecular levels were evaluated.

MATERIAL AND METHODS

Animals and experimental procedure

Twenty-week-old SHRs and their normotensive WKYs counterparts were obtained from JANVIER LABS France. Rats were group-housed 2–3 per cage. Between 28 and 51 weeks of age, cardiac function and anatomy were regularly analyzed by sequential echocardiography. BP was measured with the tail-cuff method. Male SHRs were compared with their WKYs controls throughout the study. In 28-week-old animals, diastolic function was analyzed in SHRs before and after BP reduction with a 3 mg/kg intraperitoneal injection of the calcium channel blocker, nicardipine (Aguettant, Lyon, France).

At the end of the study, all the animals were anesthetized with sodium pentobarbital for ECG recordings and LV catheterization. Before euthanasia by a pentobarbital overdose, blood was collected via a jugular venous catheter. Plasma was obtained by centrifugation and stored at −80°C until use. The heart was immediately excised and weighed. The apex was flash frozen in liquid nitrogen and stored at −80°C until use. The remaining part of the heart was fixed in 4% paraformaldehyde PBS solution.

The animal facilities are legally registered for animal housing and experimentation, and the scientists in charge of the experiments are in possession of the certificate authorizing experimentation on living animals, delivered by the governmental veterinary office. All procedures were performed in accordance with the guidelines for animal experimentation of the European Communities Council Directive EU/63/2010.

Blood pressure measurements

Systolic arterial pressure (SAP) and heart rate (HR) were taken in the morning (0800 h) by means of a noninvasive automatic BP device (Letica LE2002, Spain) after previous 5-min long heat-induced tail artery vasodilatation, in a small heating room (36–37°C) (Letica LE5610, Spain), the rat being placed in an adapted restrainer. The mean value of five readings from each animal was considered.

Echocardiography and Doppler

To allow rapid recovery from anesthesia, transthoracic echocardiography was performed in rats anesthetized with 1.5–2% isoflurane using a Sonos 5500 (Philips, USA) equipped with a 12-MHz sectorial transducer. Short-axis and long-axis views and four and five-chamber apical cardiac views were used for measurements by a sonographer blinded to the experimental groups (H.M.). End-diastolic (EDLVD) and end-systolic (ESLVD) left-ventricular diameters, diastolic posterior (PW) and septal (SW) wall thicknesses were obtained from M-mode tracings of the LV in the long-axis view. Left-atrial area was measured from the four-chamber apical view, excluding left auricle. LV weight (LVW) was calculated as $LVW = 1.04 \times [(EDLVD + PW + SW)^3 - EDLVD^3]$. The LV systolic function was analyzed by axial and longitudinal components. Shortening fraction (SF) was calculated as SF = (EDLVD−ESLVD)/EDLVD. Systolic lateral mitral annulus movement (lateral Sa) and systolic posterior wall movement (septal Sa) were obtained from the apical view using pulsed Doppler tissue imaging. The evaluation of LV diastolic function was performed with indexes taken from the four-chamber apical view. Mitral inflow was recorded by placing the pulsed Doppler window at the tip of the mitral valve. We measured maximal velocities of the E and A waves to obtain ratio E/A and the deceleration time of the E wave. The isovolumetric relaxation time (IVRT) was defined as the interval between aortic closure and the start of mitral flow. Early mitral flow propagation velocity (V_p) was assessed using color M-mode Doppler of the mitral flow. Early motion of the mitral annulus was obtained at its septal (E_{pw}) and lateral (E_m) corners by pulsed Doppler tissue imaging. LV filling index (E/E_m) was calculated. All measured and calculated indexes were presented as the average of three consecutive beats.

ECG

All measurements were obtained in sodium pentobarbital anesthetized rats (50 mg/kg, ip). After induction of the anesthesia, rats were placed in dorsal position and recorded with the four arms of the ECG leads attached at the origin of each paw by unipolar and bipolar lead derivations with an ECG (CardioMax FX-3010 Fukuda Denshi). P wave duration and amplitude, PR interval, QRS maximal amplitude, QRS duration, QT interval and ischemic changes (T wave and ST-segment amplitudes) were determined manually. We calculated corrected QT interval (QT_c) using Bazett's formula ($QT_c = QT/\sqrt{RR\ interval}$).

Invasive left-ventricular catheterization

All measurements were made in rats anesthetized with sodium pentobarbital (50 mg/kg, ip) after ECG recording.

This anesthetic induces similar effects on the cardiac diastolic function, BP and HR than isoflurane [10,11]. It was selected here to permit carotid artery catheterization in the absence of a mask delivering isoflurane. Animals were placed on a thermometer controlled heating rug (Harvard Apparatus, USA), tracheotomized and left on spontaneous breathing. A physiological saline-filled polyethylene catheter was introduced into the left ventricle through the right carotid artery and connected to a Statham Db23 transducer, which was in turn connected to a data acquisition and storage system (IOX, EMKA Technologies, France). From LV tracings, LV systolic (LVSP) and end-diastolic pressures (LVEDP) were measured. The first derivative of LV pressure was calculated. Its maximal (dP/dt_{max}) and minimal (dP/dt_{min}) values were respectively used to assess LV contractility and relaxation. Then, the catheter was slowly withdrawn, its tip being placed in the ascending aorta to obtain central systolic (SAP) and diastolic (DAP) arterial pressure during 5 min after stabilization.

Histology

The basal part of the heart, 2 mm far from mitral annulus, was fixed, paraffin-embedded and sectioned (5 μm) using standard techniques. Interstitial and perivascular myocardial collagen contents were analyzed on picro-Sirius red stained paraffin sections.

Cardiac images were captured with the aid of a light camera-equipped microscope, with a 10-fold magnification for coronary arteries and five-fold magnification for larger myocardial areas. For each rat's cardiac slice, two images of different focal fibrosis areas and two images outside these areas were recorded for interstitial fibrosis measurements. Four coronary arteries pictures were taken for perivascular fibrosis assessment. Interstitial fibrosis detection was performed using a color threshold method under Image J software, marking the red stained collagen fibers and then converting it into a pixel number. Interstitial fibrosis was then normalized by the total surface (in pixels) of the analyzed region and expressed in percentage. The epicardium, coronary vessels and papillary muscles were removed from the images before quantification. Perivascular fibrosis was measured by surface assessment of the regions of interest under Image J software. Perivascular fibrosis was expressed as the ratio of the surface of the adventitia layer on the surface of the vessel (lumina + media + adventitia). Large and medium coronary arteries (diameter of lumina + media > 130 μm; mean 170 ± 24 μm) and small coronary arteries (diameter of lumina + media <130 μm; mean 85 ± 18 μm) were considered separately.

Gene expression by reverse transcription qPCR

Total mRNA was extracted from rat cardiac apex using RNeasy Mini Kit QIAGEN (Courtaboeuf, France). The concentration of total RNA was determined by ultraviolet spectrophotometry at 260/280 nm. The cDNA were obtained by reverse transcription using Kit iScript cDNA Synthesis BioRad (Marnes-la-Coquette, France). Semi-quantitative reverse transcription-PCR was produced on an amplification system (PCR Light CyclerCaroussel) with the kit LightCycler FastStart DNA Master Plus SYBR Green I (Roche Diagnostics, Meylan, France). Table 1 shows forward and reverse primer sequences for all analyzed genes except primers encoding metalloproteases (MMPs 2, 7 and 9) that were obtained from Qiagen. For each gene, the expression data were normalized to an endogenous control glyceraldehyde-3-phosphate dehydrogenase. The reactions were considered in duplicate, and the mRNA levels of each gene were calculated according to the formula $2^{-\Delta\Delta CP}$, where in ΔCP is the difference in crossing point (CP) values between the target and the endogenous control.

Brain natriuretic plasma measurements

Brain natriuretic plasma (BNP) concentrations were determined using Multiplex and a standard rat BNP kit (Millipore, USA).

Zymography

Forty-four-week-old WKYs ($n = 4$) and SHRs ($n = 4$) were used for the experiments. Heart was collected immediately after euthanasia (100 mg/kg sodium pentobarbital i.p.), rinsed in PBS on ice. Atria were separated from ventricles and ventricular tissue frozen. Ventricular tissue (0.5 g/ml) was homogenized on ice in cold buffer (50 mmol/l Tris-HCl pH 7.5, 50 mmol/l NaCl, 2% triton) and centrifuged (10000 *g*, 4°C, 10 min). Supernatant was collected, and protein concentration was measured (BC protein assay). Thirty micrograms of proteins were added to a double volume zymogram sample buffer (Biorad, Hercules, California). Samples were subjected to 10% zymogram gelatin gel and 12.5% zymogram casein gel (BioRad) as extensively described previously [12]. Gelatinases were detected as clear bands against a dark blue background. Images were acquired and quantified using a BioRad software package (Biorad Molecular Imager, ImageLab™ software, Marnes-la-Coquette, France).

Data analysis and statistics

All the values were expressed as mean ± SD. Statistical comparisons between two or more groups were performed when appropriate using Student's unpaired *t* tests

TABLE 1. Primers sequences of the seven genes analyzed

Gene	Primer	Sequences (5′-3′)
GAPDH	Forward	GCAAGAGAGAGGCCCTCAG
	Reverse	TGTGAGGGAGATGCTCAGTG
β-MHC	Forward	TGTCCAAGTTCCGCAAGGT
	Reverse	CAAGATCTACTCTTCATTCAGGCC
BNP	Forward	CTGTGACGGGCTGAGGTTGT
	Reverse	TGGCAAGTTTGTGCTGGAAG
ANP	Forward	TGAGCCGAGACAGCAAACA
	Reverse	TCCAGGTGGTCTAGCAGGTT
Collagen 1a	Forward	ACGCATGGCCAAGAAGACATC
	Reverse	TTTGCATAGCACGCCATCG
Collagen 3a	Forward	CAGCTGGCCTTCCTCAGACTT
	Reverse	GCTGTTTTTGCAGTGGTATGTAATGT
SERCA 2a	Forward	ATCTTTCGTTTTGGCTTGGTT
	Reverse	CATTTTCAGCGTTTCTCTCCT

ANP, atrial natriuretic peptide; BNP, brain natriuretic peptide; GAPDH, glyceraldehyde-3-phosphate dehydrogenase; β-MHC, β-myosin heavy chain; SERCA 2a, sarco/endoplasmic reticulum calcium ATPase 2a.

or two-way repeated measures-ANOVA followed by post-hoc analysis with Bonferroni's test (GraphPad Prism Software version 6.0, San Diego, California, USA). $P < 0.05$ was considered statistically significant.

RESULTS

Blood pressure, heart rate, body weight and cardiac geometric remodeling

All along the study (20 weeks old to 52–53 weeks old), SHRs demonstrated severe hypertension and tachycardia (Table 2). SHRs body weight was lower than the age-matched WKYs (Table 2). The high arterial pressure induced cardiac hypertrophy as demonstrated by echocardiography (Table 3), direct cardiac mass measurement (2.2 ± 0.2 g in SHRs versus 1.4 ± 0.1 g in WKYs, $P < 0.05$), cardiac mass to body weight ratio (4.9 ± 0.5 g/kg in SHRs versus 2.9 ± 0.6 g/kg in WKYs, $P < 0.05$) and the increase of the ECG QRS maximal amplitude (1080 ± 240 μV in SHRs versus 450 ± 100 μV in WKYs, $P < 0.05$). This LV hypertrophy appeared as concentric because LV septum and posterior wall thicknesses were significantly increased, whereas LV end-diastolic and end-systolic diameters were not modified (Table 3). At the end of the observation period (53-week-old animals), the cardiac hypertrophy was confirmed by an increased β-myosin heavy chain gene expression (ΔCP: 9 ± 0.9 in SHRs versus 11 ± 1.2 in WKYs, $P < 0.05$). From the 28-week-old time-point onward, a progressive increase in the left-atrial area was observed in SHRs (Table 3).

Spontaneously hypertensive rats show a long-lasting diastolic dysfunction turning progressively to left-ventricular increased filling pressures

At no time-point of the follow-up in baseline conditions, we identified any patent systolic dysfunction in SHRs as attested by normal LV-shortening fraction and systolic mitral annulus movement (Sa) measured by Doppler tissue imaging (Table 3).

However, we identified an augmentation of E/A ratio (Fig. 1a) and an alteration of the early LV diastole in SHRs. An increase of the IVRT was observed in 20-week-old animals (Fig. 1b). In 28-week-old SHRs and later, Doppler tissue imaging at the mitral annulus confirmed this diastolic dysfunction showing a decrease in the early diastolic velocities (Fig. 1c, d). V_p was not modified in SHRs (Table 3).

To test the afterload dependence of these alterations, we measured all the echocardiographic parameters before and 8 h after the intraperitoneal injection of the calcium blocker, nicardipine. This drug induced an important and significant BP reduction (198 ± 10 mmHg before versus 144 ± 14 mmHg after, $P < 0.01$). A significant tachycardia was also simultaneously observed (388 ± 52 bpm before versus 443 ± 45 bpm after, $P < 0.01$). BP reduction completely normalized the E/A ratio (1.8 ± 0.4 before versus 1.3 ± 0.1 after, $P > 0.05$) attesting of the BP dependence of this parameter in rats. However, tissue Doppler imaging parameters at the lateral (E_m: 3.5 ± 1.1 cm/s before versus 4 ± 0.2 cm/s after, $P > 0.05$) and septal (E_{pw}: 4.5 ± 0.8 cm/s before versus 4 ± 0.2 cm/s after, $P > 0.05$) corners of the mitral annulus were still altered despite the BP reduction. As a consequence, the E/E_m ratio was reduced but not normalized by the BP reduction (42 ± 3 before versus 32 ± 2 after, $P < 0.05$ compared with WKYs). Similarly, the increased IVRT observed in SHRs was not normalized by nicardipine (22 ± 3 ms before versus 23 ± 3 ms after, $P > 0.05$ compared with WKYs). As shown before, V_p was not modified in SHRs compared with WKYs and not affected by the BP reduction (data not shown).

At the end of the observation period, invasive LV catheterization confirmed the absence of systolic dysfunction in SHRs in baseline condition. On the contrary, probably because of the high BP (SAP: 171 ± 28 mmHg in SHRs versus 99 ± 37 mmHg in WKYs, $P < 0.05$; DAP: 115 ± 31 mmHg in SHRs versus 76 ± 37 mmHg in WKYs, $P < 0.05$), a significant increase in dP/dt_{max} was observed in 53-week-old animals (8584 ± 3281 mmHg/s in SHRs versus 5207 ± 1609 mmHg/s in WKYs, $P > 0.05$). The maximal speed of relaxation as measured by the dP/dt_{min} parameter was also not affected (-6906 ± 2375 mmHg/s in SHRs versus -4392 ± 2287 mmHg/s in WKYs, $P > 0.05$). The less load-dependent relaxation index, dP/dt_{min}/LVSP (LVSP: left-ventricular systolic pressure) was not modified in SHRs ($49 \pm 15\ s^{-1}$ in SHRs versus $46 \pm 14\ s^{-1}$ in WKYs, $P > 0.05$). In these anesthetized conditions, LVEDP was slightly increased in SHRs (16 ± 6 mmHg versus 11 ± 3 mmHg in WKYs). This last result confirmed what had been observed with the noninvasive echocardiographic E/E_m parameter and RT-qPCR analysis in 53-week-old myocardial samples in which we showed augmentation of BNP and atrial natriuretic peptide (ANP) genes expression (ΔCP: 11 ± 1 in SHRs versus 14.5 ± 0.7 in WKYs, $P < 0.01$ for BNP and 9.8 ± 1 in SHRs versus 15.2 ± 2.1 in WKYs, $P < 0.01$ for ANP). At the plasma level, BNP was also increased in SHRs (69 ± 25 pg/ml in SHRs versus 23 ± 17 pg/ml in WKYs, $P < 0.05$). The sarco/endoplasmic reticulum calcium ATPase 2a (SERCA 2a) gene expression was not modified (data not shown).

TABLE 2. Blood pressure, heart rate and body weight measurements in spontaneously hypertensive rats and Wistar–Kyoto rats

	WKYs			SHRs		
	28 WO	43 WO	51 WO	28 WO	43 WO	51 WO
SAP (mmHg)	118 ± 8	120 ± 11	121 ± 11	$195 \pm 14^*$	$179 \pm 12^*$	$192 \pm 11^*$
HR (bpm)	347 ± 36	335 ± 50	340 ± 47	$393 \pm 50^*$	$402 \pm 54^*$	$411 \pm 60^*$
BW (g)	459 ± 10	496 ± 64	495 ± 92	$407 \pm 15^*$	$456 \pm 16^*$	462 ± 21

BW, body weight; HR, heart rate; SAP, systolic arterial pressure; WKYs, Wistar–Kyoto rats; WO, week old.
$^*P < 0.05$ versus WKYs of the same age.

TABLE 3. Echocardiographic longitudinal follow-up of Wistar–Kyoto rats and spontaneously hypertensive rats (28–51 weeks old)

	WKY					SHR				
	28 WO	36 WO	43 WO	47 WO	51 WO	28 WO	36 WO	43 WO	47 WO	51 WO
EDLVD (mm)	7.45 ± 0.36	7.97 ± 0.69	8.4 ± 0.4	8.1 ± 0.7	8.5 ± 0.4	7.0 ± 0.4	7.35 ± 0.46	7.8 ± 0.5**	8.1 ± 0.5**	8.6 ± 0.5**
ESLVD (mm)	3.1 ± 0.6	3.83 ± 0.82	4.2 ± 0.5	4.08 ± 0.8	4.2 ± 0.6	2.8 ± 0.6	3.3 ± 0.6**	3.6 ± 0.5**	3.82 ± 0.36**	4.6 ± 0.5**
SWT (mm)	1.53 ± 0.06	1.56 ± 0.06	1.56 ± 0.06	1.4 ± 0.1	1.38 ± 0.07	1.89 ± 0.01*	1.92 ± 0.01*	2 ± 0.08*,**	2.02 ± 0.06*,**	2.1 ± 0.1*,**
PWT (mm)	1.50 ± 0.07	1.53 ± 0.05	1.55 ± 0.08	1.40 ± 0.08	1.4 ± 0.1	1.81 ± 0.07*	1.83 ± 0.08*	1.95 ± 0.07*,**	1.96 ± 0.08*,**	2.03 ± 0.07*,**
LV mass (mg)	769 ± 96	885 ± 126	967 ± 47	802 ± 81	868 ± 84	920 ± 101*	1017 ± 119*	1206 ± 141*,**	1286 ± 125*,**	1497 ± 163*,**
LV mass index (mg/g)	1.68 ± 0.22	2.22 ± 0.25	1.97 ± 0.33	1.66 ± 0.33	1.72 ± 0.26	2.26 ± 0.28*	2.37 ± 0.28	2.6 ± 0.3*	2.75 ± 0.27*,**	3.25 ± 0.38*,**
SF (%)	58.6 ± 7.7	52.3 ± 7.3	51 ± 4	49.9 ± 7.2	51 ± 6	60 ± 7.3	55 ± 7.6	53 ± 5	53 ± 6	46 ± 6**
Lateral S wave (cm/s)	7.1 ± 1.4	7.63 ± 1.5	7.09 ± 1.23	6.7 ± 1.3	6.78 ± 1.23	6.1 ± 1.1	6.9 ± 1.1	7.46 ± 1.37	7.06 ± 1.04	6.54 ± 1.04
E wave (cm/s)	113 ± 10	111 ± 14	101 ± 16	99 ± 18	112 ± 17	127 ± 14	128 ± 19	131 ± 21*	145 ± 17*	140 ± 20*
A wave (cm/s)	95 ± 9	85 ± 11	90 ± 8.5	79.6 ± 16.4	93 ± 11	82.7 ± 21.3	89.7 ± 20.5	91 ± 18	98 ± 27	96 ± 30
V_p (cm/s)	23.3 ± 3.9	25.4 ± 2.6	24.6 ± 1.9	25.7 ± 2.5	26.2 ± 3.6	21.7 ± 4.6	21.5 ± 2.6	25 ± 3	24 ± 2.3	25 ± 2.9
E/E_m	18.7 ± 3.3	18.3 ± 3.1	17.2 ± 2.9	18.4 ± 2.5	19.3 ± 2.3	32.7 ± 9.0*	30.5 ± 6.0*	33.6 ± 8.5*	32.6 ± 4.8*	32 ± 3*
TS LA area (cm^2)	0.29 ± 0.02		0.29 ± 0.05	0.25 ± 0.05	0.25 ± 0.03	0.31 ± 0.04		0.38 ± 0.04*,**	0.42 ± 0.05*,**	0.42 ± 0.03*,**

E, maximal velocity of mitral E wave; EDLVD, end diastolic left-ventricular diameter; E_m, early diastolic velocities at the lateral portion of mitral annulus in Doppler tissue imaging; ES LA area, end systolic left atrium area; ESLVD, end systolic left-ventricular diameter; LV mass, left-ventricular mass; PWT, posterior wall thickness; SF, shortening fraction; SWT, septum wall thickness; V_p, protodiastolic propagation of E wave flow in M-mode; WO, week old.
*$P < 0.05$ versus WKY of same age.
**$P < 0.05$ versus 28-week-old SHR; two-way RM-ANOVA; values are expressed as mean ± SD.

Electrical remodeling and myocardial ischemia in old spontaneously hypertensive rats

In 53-week-old SHRs, ECG identified conduction and repolarization abnormalities. Indeed, a prolongation of the PR interval was observed in SHRs (52 ± 3 ms versus 41 ± 5 ms in WKYs, $P < 0.05$). A longer QRS duration was also noticed in SHRs (43 ± 8 ms versus 18 ± 2 ms in WKYs, $P < 0.05$). These hypertensive animals exhibited some disorders of the ventricular repolarization as shown by the QT (107 ± 8 ms versus 83 ± 11 ms in WKYs, $P < 0.05$) and QTc interval prolongations (258 ± 15 ms versus 190 ± 15 ms in WKYs, $P < 0.05$). Interestingly, a decrease in T wave amplitude (0.04 ± 0.08 mV in SHRs versus 0.16 ± 0.08 mV in WKYs, $P = 0016$) and a decrease in ST-segment amplitude (0.004 ± 0.08 mV in the SHRs versus 0.08 ± 0.05 mV in WKYs, $P = 0.049$) were demonstrated in SHRs. The modifications could argue in favor of subendocardial myocardial ischemia and lesions. Finally, the P wave

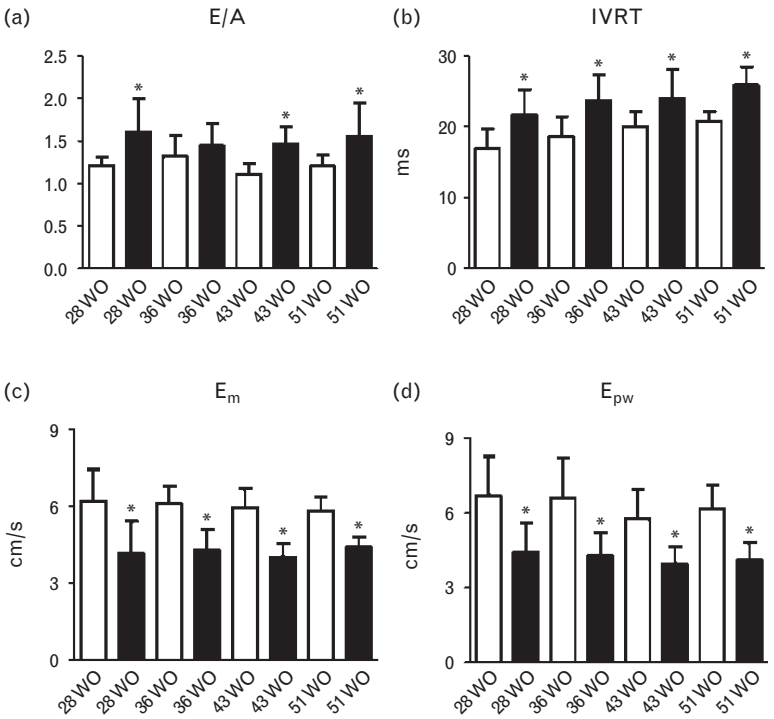

FIGURE 1 Main echocardiographic diastolic parameters modified in SHRs. In 51-week-old SHRs, a diastolic dysfunction was demonstrated by an increase of the E/A ratio (a) and IVRT (b). At the same time-point, Doppler tissue imaging showed a decrease of the mitral annulus motion at its lateral (c) and septal (d) corners. *$P < 0.05$ versus WKYs of the same age. Open box: WKYs, black box: SHRs. IVRT, isovolumetric relaxation time; SHRs, spontaneously hypertensive rats; WKYs, Wistar–Kyoto rats.

analysis confirmed atrial remodeling observed with echocardiography. P wave increased in duration (24 ± 4 ms in SHRs versus 19 ± 1 ms in WKYs, $P < 0.05$) as well as in amplitude (83 ± 26 μV in SHRs versus 40 ± 20 μV in WKYs, $P < 0.05$).

Left-ventricular myocardial collagen deposit

In SHRs, an increase in LV myocardial collagen content was observed. RT-qPCR revealed an increased collagen 1a and 3a mRNA expression (Fig 2a, b). Collagen deposition was mainly localized in the subendocardial LV free wall layers (Fig. 2c, e). At this level, an augmentation of collagen was also noticed in the adventitia of small coronary arteries (Fig. 2d, f). Concerning large and medium coronary arteries, perivascular collagen deposition was not significantly modified in these old SHRs (data not shown).

To analyze extracellular matrix turnover, we investigated MMPs 2, 7 and 9 at the expression (mRNA) and functional (zymography) levels in ventricles from 44-week-old WKYs and SHRs. RT-qPCR identified an overexpression of MMP-2 [$2^{-\Delta\Delta cp}$ 2.78 (1.88–4.11); $P < 0.05$ versus WKYs] but no significant change for MMP-9 [$2^{-\Delta\Delta cp}$ 2.03 (1.57–6.49); $P > 0.05$ versus WKYs. mRNA encoding MMP-7 was detected but at very low levels making quantification uncertain. At the functional level, no change was observed concerning MMPs 2 and 9, but a two times increase in MMP-7 activity was detected (Fig. 3).

DISCUSSION

In the present work, we have shown that, in combination with high BP and LV hypertrophy, SHRs develop a progressive alteration of the diastolic function mainly

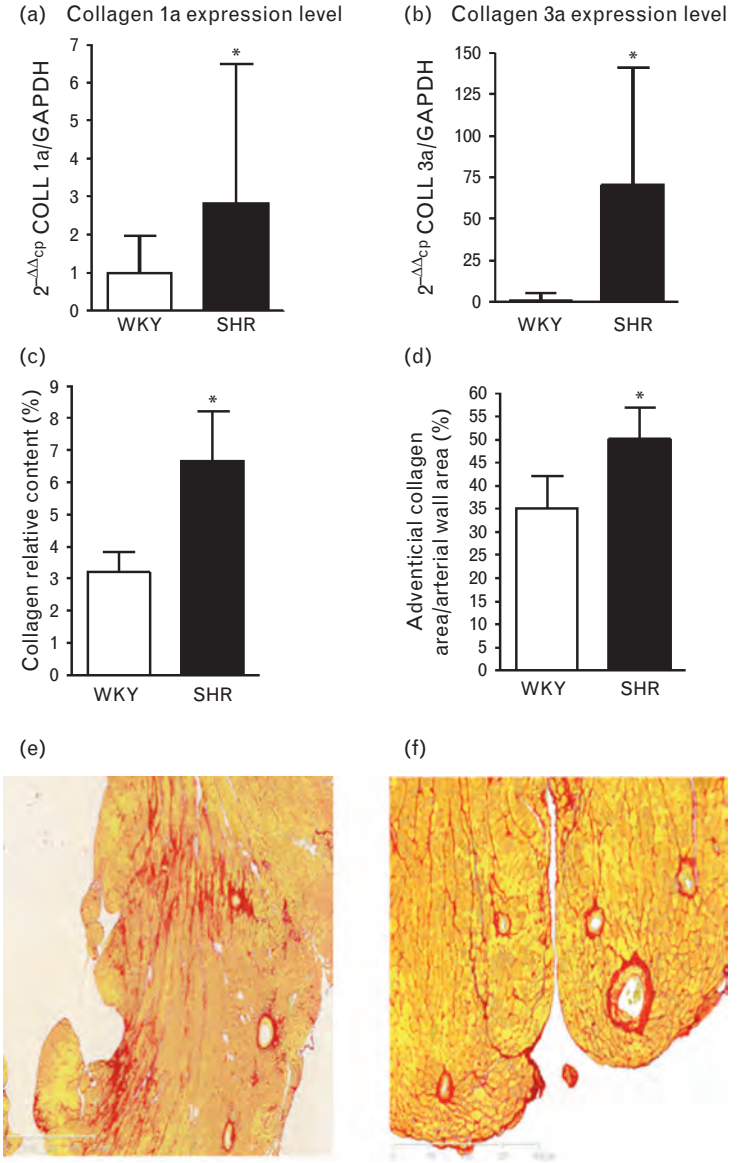

FIGURE 2 Left-ventricular fibrosis analyzed by RT-qPCR and histology. In 53-week-old SHRs, collagen 1a (a) and 3a (b) genes expression were increased. The collagen deposit was mainly observed in subendocardial layers (c, e) and small coronary arteries (d, f). *$P < 0.05$ versus WKYs of the same age. SHRs, spontaneously hypertensive rats; WKYs, Wistar–Kyoto rats; RT-qPCR, reverse transcription-qPCR.

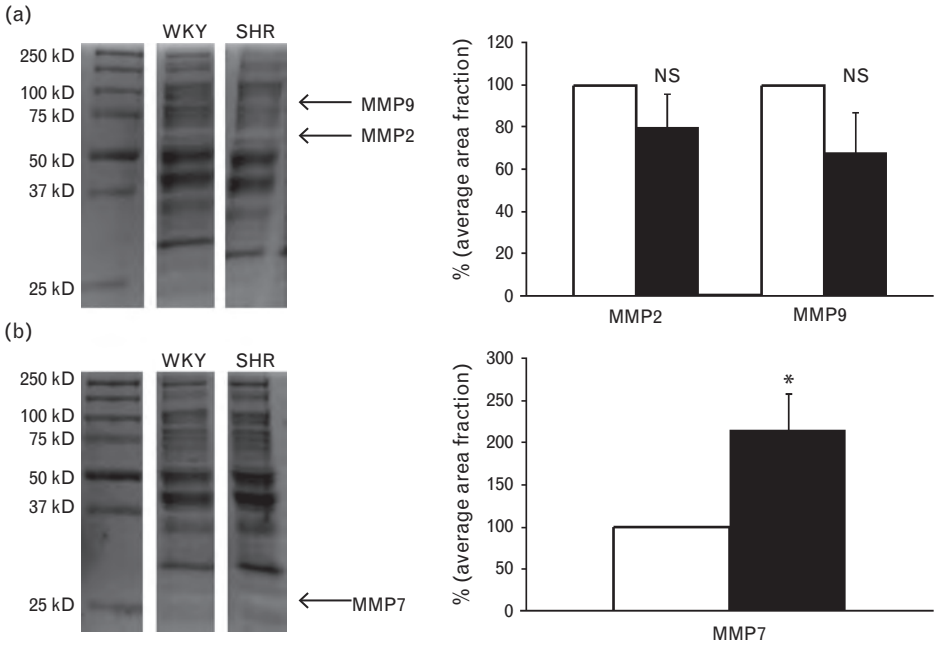

FIGURE 3 Analysis of ventricular metalloproteases 2, 7 and 9 activities by zymography in WKYs and SHRs. In 44-week-old SHRs, MMPs 2 (MW 62 kD) and 9 activities (MW 92 kD) were not significantly different (a). MMP-7 activity was increased by 2.14 times in SHRs versus WKYs (MW 28 kD) (b). Open box: WKYs, black box: SHRs. $^{*}P < 0.05$ versus WKYs of the same age. NS, not significant. MMPs, metalloproteases; MW, molecular weight; SHRs, spontaneously hypertensive rats; WKYs, Wistar–Kyoto rats.

affecting the early relaxation. Among all echocardiographic parameters, IVRT and tissue Doppler at the mitral annulus appear the most predictive for diastolic dysfunction. Around 1 year of age, these animals show a progressive increase in LV filling pressures and electrical signs of subendocardial ischemia. The last is confirmed by histology showing subendocardial focal fibrosis.

Among all rodent models of systemic hypertension, the SHR model shows many interests. It is spontaneously occurring and reveals many similarities to human essential hypertension. Indeed, despite a very high afterload level, arterial hypertension leads to long-lasting-compensated LV hypertrophy without any clinical sign of heart failure. Impaired myocardial performance occurs a long time before overt failure. Finally, most of the currently used echocardiographic parameters have been validated in adult hypertensive and normotensive rats [9–13]. But, till now, only few studies followed longitudinally the cardiac function with echocardiography in SHRs older than 3 months. As an experimental tool, this technique is fully noninvasive and offers a good reproducibility when carried out by only one trained operator blinded to the experimental groups.

In SHRs, we observed the classical high BP associated with tachycardia that probably reflects the well documented sympathetic hyperactivity both at central [14] and peripheral [15] levels, and the concentric LV hypertrophy. At a cardiac functional point of view, we also confirmed previous findings [16] dealing with an apparent preservation of the LV systolic function in SHRs, at least in baseline conditions. Global cardiac contractility measured by the index dP/dt_{max} is increased as a consequence of high BP, suggesting an increased rate of contraction because of the adequate hypertrophic response at least in the early months of the evolution. Echocardiography permits the analysis of the contraction of circular and longitudinal myocardial fibers. Circular fibers contractility is not altered because the LV-shortening fraction appears unmodified. Similarly, the contraction rate of the longitudinal fibers, which are classically more prone to decompensation than circular fibers, is also unaltered all along the study as shown by the systolic mitral annulus movement (Sa).

The observed progressive dilatation of the left atrium indirectly attests an increase of the filling pressures not due to systolic failure but to diastolic dysfunction generating a higher atrial to ventricular pressure gradient, required for proper early LV filling. This higher gradient is confirmed by the higher E wave velocity that is observed even in young animals. In fact, in young SHRs, echocardiography confirmed previous studies [9–13] by the identification of an LV filling impairment with the following four indexes IVRT, E/A, E_m and E_{pw}. In humans, IVRT appears as a load-dependent index, whereas the other parameters are relatively less dependent on loading conditions. V_p is more difficult to measure, especially in rats, and exhibits a lower intraobserver reproducibility compared with other Doppler indexes [17]. In this work, V_p is not significantly modified in SHRs. To test the load dependence of the other diastolic parameters, we reduced BP in SHRs with the calcium blocker, nicardipine. This compound was selected for its particular tropism for vascular smooth muscle cells as compared with cardiomyocytes. It induces an acute important reduction of the BP that is maximal 8 h after injection and lasts about 24 h (data not shown) and a tachycardia. Similarly to humans, the E/A ratio is normalized by the BP reduction showing its higher sensitivity to loading conditions than tachycardia that should, at the opposite, increase diastolic filling pressures and worsen the parameter. Therefore, the interpretation of a modified

E/A ratio should be made with caution in hypertensive rats. On the opposite, IVRT, E_m and E_{pw} are less sensitive to loading. But, we cannot exclude that tachycardia could, at least in part, contributes to the maintenance of the alteration of these parameters, even if the mechanism of the increased HR implies a sympathetic activation and its positive lusitropic consequences. The modification of these parameters, that mainly evaluate the early diastole, argues in favor of a reduction of the cardiomyocytes relaxation properties. Such dysfunction could appear as early as 3 weeks old in SHRs [18]. In a recent study investigating the time course of cardiac abnormalities in aortic-banded rats, Perlini *et al.* [19] identified that alterations of the early diastole predict the progression of compensated pressure overload hypertrophy to heart failure. In this rapidly progressing model associated with major LV hypertrophy, changes in early filling dynamics picked-up animals that lost, a few weeks later, the contractile response to isoproterenol despite subnormal endocardial fractional shortening. In SHRs, altered LV early filling can be the hallmark of a global ventricular dysfunction, which, very early, predicts an evolution toward heart failure. To explore if the alteration of the early diastole could be in relation with a diastolic reticulum calcium capture abnormality, we explored the SERCA 2a mRNA expression. We did not observe any change at the mRNA level compared with WKYs animals but, a recent study reported a decrease in SERCA 2a protein with unchanged SERCA 2a mRNA expression [18], leading to changes in intracellular calcium homeostasis, main cause of LV diastolic dysfunction. In the same work, at cellular level, SERCA 2a mRNA expression was not significantly modified in SHRs. Therefore, in SHRs, a decrease in SERCA 2a activity may be due to protein degradation rather than decreased mRNA expression.

At the end of the observation period (53 weeks old), invasive cardiac catheterization did not identify impaired LV relaxation with the parameters dP/dt_{min} and dP/dt_{min}/LVSP. Catheterization was performed under pentobarbital anesthesia. An effect of this barbiturate on LV diastolic and systolic functions as well as systemic vascular resistances cannot be ruled out as described in other studies [20,21].

We observed a continuous increase in LV filling pressure as attested by the follow-up of E/E_m parameter and the EDLVD measurement at the end of the study that is indirectly confirmed by the left atrium enlargement and the myocardial augmentation of ANP and BNP expression. The cardiac BNP production probably accounts for the observed increase in the plasma. This pattern is mainly due to diastolic dysfunction because we never identified restrictive filling profiles, and cardiac dysfunction appeared compensated, at least in resting conditions. An evolution toward overt heart failure could be favored by interstitial myocardial remodeling. Recent literature was interested in the link between extracellular cell matrix turnover and alteration of the early LV filling before the onset of systolic dysfunction. Clinical studies attempted to correlate myocardial fibrosis evaluated by late postgadolinium myocardial enhancement and noninvasive cardiac hemodynamics. In 204 patients, Moreo *et al.* [22] established a correlation between the degree of diastolic dysfunction and the extent of myocardial fibrosis regardless of the underlying cause. In hypertrophic cardiomyopathy, a correlation is also found between LV filling pressures and degree of fibrosis [23]. Interestingly, this cardiac disease is in fact heterogeneous. Simultaneous strain rate analysis by speckle tracking and delayed hyperenhancement MRI showed that the extent of local fibrosis detected a segmental diastolic dysfunction independently of hypertrophy [24]. This result emphasizes that diastolic dysfunction is more influenced by collagen turnover than cardiomyocyte hypertrophy itself. Nevertheless, fibrosis could also constitute a pathophysiological trigger of transition toward failure. Some studies evaluated plasma matrix MMPs in relation to Doppler-echocardiographic parameters. In the work by Martos *et al.* [25] performed in hypertensive patients, plasma MMP-2 increased in proportion to the severity of the diastolic dysfunction when MMP-9 was not affected. But, a subgroup analysis emphasized that MMPs increase was mainly observed in failing patients even for MMP-9. At the opposite, in hypertensive patients with an HF-PEF, the MMP-1/tissue inhibitor metalloprotease-1 (TIMP-1) ratio was not affected by an elevation in left-side filling pressures [26]. In experimental models, a correlation is found between diastolic dysfunction and myocardial fibrosis in senescent mice [27] but in Dahl salt-sensitive rats fed a high-salt diet, MMP-2 and MMP-9 were mainly increased when hypertrophied animals turned to overt heart failure [28]. Taken together, all the data argue in favor or a role of the extracellular cell matrix activation in the pathophysiology of diastolic dysfunction, an acceleration of the process pushing to failure. In the present work, collagen type 1a and 3a mRNA expression are intensified, a phenomenon that appears early in the development of the cardiac disease [29,30]. Nevertheless, the interstitial fibrosis is light probably affecting ventricular compliance only when filling pressures are markedly elevated. In accordance with these assumptions, we were unable to identify a clear increase in MMP-2 activity despite a significant augmentation of mRNA expression, and no change was observed concerning the MMP-9 subtype neither at the protein activity nor at expression level. This pattern of MMP-2 expression and activity could be the hallmark of heart failure with preserved ejection fraction. In a previous study performed in aortic-banded Guinea pigs, Tozzi *et al.* [31] have demonstrated that in animals showing an increase in LV filling pressures and a normal endocardial fractional shortening, the MMP-2 activity was apparently normal probably because of an augmentation of TIMP-2 myocardial concentration. This heart failure pattern was observed in parallel with myocardial fibrosis and is quite similar to the one we observed in 53-week-old SHRs. Interestingly, collagen deposition is mainly localized in the subendocardium of the LV free wall as described in other studies [32,33]. This particular location could be the consequence of the particular coronary circulation in rats, showing large septal coronary artery branches. Moreover, we show growing perivascular collagen deposition only in small coronary vessels. In this model, the demonstration of an MMP-7 ventricular overactivity could be the hallmark of this preferential location of fibrosis around coronary arteries because this subtype is mainly localized in rat arterial wall. We hypothesized that these alterations of the

subendocardial coronary microcirculation could drive to myocardial ischemia and, in some cases, necrosis. To verify this hypothesis, we performed ECG just before LV catheterization at the end of our study. We confirmed previous data showing intracardiac conduction abnormalities, such as PR prolongation and QRS enlargement [34,35]. The last could also be due to both cardiac hypertrophy and interstitial fibrosis. In addition, we validated the hypothesis of spontaneous myocardial ischemia in old SHRs by the identification of QTc prolongation and ST segment decrease or elevation compatible with ischemic changes. We corroborated some previous data [36,37], but the link between these ischemic changes and the future hemodynamic evolution has still to be established. The result of a complex pattern of alterations associating high BP, increased heart weight, ventricular remodeling (myocyte hypertrophy and interstitial fibrosis) and structural alterations of the coronary microcirculation could induce these ECG abnormalities.

To conclude, the old SHR appears as a model that summarizes numerous cardiac alterations observed in HF-PEF, and these are hypertension, LV hypertrophy and apparently normal contractility. Some echocardiographic parameters appear independent of loading conditions and could be used for the evaluation of drugs acting on the early diastole even if they reduce BP.

ACKNOWLEDGEMENTS

The authors would like to thank all the sponsors of this work (Fondation de France, University of Strasbourg, Centre Hospitalier et Universitaire de Strasbourg, Agence Nationale pour la Recherche). Claudia de Tapia (Laboratoire de Neurobiologie et Pharmacologie Cardiovasculaire), Patrice Goetz-Reiner and Isabelle Tilly (Mouse Clinical Institute) are thanked for their technical assistance.

Conflicts of interest

The authors declare no conflicts of interest.

REFERENCES

1. McMurray JJ, Adamopoulos S, Anker SD, Auricchio A, Böhm M, Dickstein K, *et al.* ESC Guidelines for the diagnosis and treatment of acute and chronic heart failure 2012. *Eur Heart J* 2012; 33:1787–1847.
2. Cleland JG, Swedberg K, Follath F, Komajda M, Cohen-Solal A, Aguilar JC, *et al.* The EuroHeart Failure survey programme a survey on the quality of care among patients with heart failure in Europe. Part 1: patient characteristics and diagnosis. *Eur Heart J* 2003; 24:442–463.
3. Lenzen MJ, Scholte op Reimer WJ, Boersma E, Vantrimpont PJ, Follath F, Swedberg K, *et al.* Differences between patients with a preserved and a depressed left ventricular function: a report from the EuroHeart Failure Survey. *Eur Heart J* 2004; 25:1214–1220.
4. Yusuf S, Pfeffer MA, Swedberg K, Granger CB, Held P, McMurray JJ, *et al.* Effects of candesartan in patients with chronic heart failure and preserved left-ventricular ejection fraction: the CHARMPreserved Trial. *Lancet* 2003; 362:777–781.
5. Massie BM, Carson PE, McMurray JJ, Komajda M, McKelvie R, Zile MR, *et al.* Irbesartan in patients with heart failure and preserved ejection fraction. *N Engl J Med* 2008; 359:2456–2467.
6. Gomes AC, Falcão-Pires I, Pires AL, Brás-Silva C, Leite-Moreira AF. Rodent models of heart failure: an updated review. *Heart Fail Rev* 2013; 18:219–249.
7. Litwin SE, Katz SE, Morgan JP, Douglas PS. Serial echocardiographic assessment of left ventricular geometry and function after large myocardial infarction in the rat. *Circulation* 1994; 89:345–354.
8. Ono K, Masuyama T, Yamamoto K, Doi R, Sakata Y, Nishikawa N, *et al.* Echo Doppler assessment of left ventricular function in rats with hypertensive hypertrophy. *J Am Soc Echocardio* 2002; 15:109–117.
9. Slama M, Ahn J, Varagic J, Susic D, Frohlich ED. Long-term left ventricular echocardiographic follow-up of SHR and WKY rats: effects of hypertension and age. *Am J Physiol Heart Circ Physio* 2004; 286:181–185.
10. Zuurbier CJ, Keijzers PJM, Koeman A, Van Wezel HB, Hollmann MW. Anesthesia's effects on plasma glucose and insulin and cardiac hexokinase at similar hemodynamics and without major surgical stress in fed rats. *Anesth Analg* 2008; 106:135–142.
11. Stein AB, Tiwari S, Thomas P, Hunt G, Levent C, Stoddart MF, *et al.* Effects of anesthesia on echocardiographic assessment of left ventricular structure and function in rats. *Basic Res Cardiol* 2007; 102:28–41.
12. Hu X, Beeton C. Detection of functional matrix metalloproteinases by zymography. *J Vis Exp* 2010; 45:e2445.
13. Slama M, Ahn J, Peltier M, Maizel J, Chemla D, Varagic J, *et al.* Validation of echographic and Doppler indexes of left ventricular relaxation in adult hypertensive and normotensive rats. *Am J Physiol Heart Circ Physiol* 2005; 289:1131–1136.
14. Judy WV, Farrell SK. Arterial baroreceptor reflex control of sympathetic nerve activity in the spontaneously hypertensive rat. *Hypertension* 1979; 1:605–614.
15. Li D, Wang L, Lee CW, Dawson TA, Paterson DJ. Noradrenergic cell specific gene transfer with neuronal nitric oxide synthase reduces cardiac sympathetic neurotransmission in hypertensive rats. *Hypertension* 2007; 50:69–74.
16. Cingolani OH, Yang XP, Cavasin MA, Carretero OA. Increased systolic performance with diastolic dysfunction in adult spontaneously hypertensive rats. *Hypertension* 2003; 41:249–254.
17. Slama M, Susic D, Varagic J, Ahn J, Frohlich ED. Echocardiographic measurement of cardiac output in rats. *Am J Physiol Heart Circ Physio* 2003; 284:691–697.
18. Dupont S, Maizel J, Mentaverri R, Chillon JM, Six I, Giummelly P, *et al.* The onset of left ventricular diastolic dysfunction in SHR rats is not related to hypertrophy or hypertension. *Am J Physiol* 2012; 302:1524–1532.
19. Perlini S, Chung ES, Aurigemma GP, Meyer TE. Alterations in early filling dynamics predict the progression of compensated pressure overload hypertrophy to heart failure better than abnormalities in midwall systolic shortening. *Clin Exp Hypert* 2013; 35:401–411.
20. Smith TL, Hutchins PM. Anesthetic effects on hemodynamics of spontaneously hypertensive and Wistar-Kyoto rats. *Am J Physiol Heart Circ Physiol* 1980; 238:539–544.
21. Janssen BJ, De Celle T, Debets JJ, Brouns AE, Callahan MF, Smith TL. Effects of anesthetics on systemic hemodynamics in mice. *Am J Physiol Heart Circ Physiol* 2004; 287:1618–1624.
22. Moreo A, Ambrosio G, De Chiara B, Tran T, Mauri F, Raman SV. Influence of myocardial fibrosis on left ventricular diastolic function. Noninvasive assessment by cardiac magnetic resonance and echo. *Circ Cardiovasc Imaging* 2009; 2:437–443.
23. Ellims AH, Iles LM, Ling L, Hare JL, Kaye DM, Taylor AJ, *et al.* Diffuse myocardial fibrosis in hypertrophic cardiomyopathy can be identified by cardiovascular magnetic resonance, and is associated with left ventricular diastolic dysfunction. *J Cardiovasc Magn Res* 2012; 14:76.
24. Chang SA, Lee SC, Choe YH, Hahn HJ, Jang SY, Park SJ, *et al.* Effects of hypertrophy and fibrosis on regional and global functional heterogeneity in hypertrophic cardiomyopathy. *Int J Cardiovasc Imaging* 2012; 28:133–140.
25. Martos R, Baugh J, Ledwidge M, O'Loughlin C, Conlon C, Patle A, *et al.* Diastolic heart failure. Evidence for increased myocardial collagen turnover linked to diastolic dysfunction. *Circulation* 2007; 115:888–895.
26. Gonzales A, Lopez B, Querejeta R, Zubillaga E, Echeverria T, Diez J. Filling pressures and collagen metabolism in hypertensive patients with heart failure and normal ejection fraction. *Hypertension* 2010; 55:1418–1424.
27. Reed AL, Tanaka A, Sorescu D, Liu H, Jeong EM, Sturdy M, *et al.* Diastolic dysfunction is associated with cardiac fibrosis in the senescence-accelerated mouse. *Am J Physiol Heart Circ Physiol* 2011; 301:H824–H831.
28. Ichihara S, Noda A, Nagata K, Obata K, Xu J, Ichihara G, *et al.* Pravastatin increases survival and suppresses an increase in myocardial

matrix metalloproteinase activity in a rat model of heart failure. *Cardiovasc Res* 2006; 69:726–735.
29. Bing OH, Conrad CH, Boluyt MO, Robinson KG, Brooks WW. Studies of prevention, treatment and mechanisms of heart failure in the aging spontaneously hypertensive rat. *Heart Fail Rev* 2002; 7:71–88.
30. Boluyt MO, Bing OHL. Matrix gene expression and decompensated heart failure: the aged SHR model. *Cardiovasc Res* 2000; 46:239–249.
31. Tozzi R, Palladini G, Fallarini S, Nano R, Gatti C, Presotto C, *et al*. Matrix metalloprotease activity is enhanced in the compensated but not in the decompensated phase of pressure overload hypertrophy. *Am J Hypert* 2007; 20:663–669.
32. Belichard P, Pruneau D, Brown NL, Salzmann JL, Rouet R. Hypertensive myocardial hypertrophy an rhythm disorders: 2 possible origins. *Arch Mal Coeur Vaiss* 1989; 82:1303–1308.
33. Bing OH, Ngo HQ, Humphries DE, Robinson KG, Lucey EC, Carver W, *et al*. Localization of α1(I) collagen mRNA in myocardium from the spontaneously hypertensive rat during the transition from compensated hypertrophy to failure. *J Mol Cell Cardiol* 1997; 29:2335–2344.
34. Bacharova L, Kyselovic J, Klimas J. QRS voltage-duration product in the identification of left ventricular hypertrophy in spontaneously hypertensive rats. *Arq Bras Cardiol* 2002; 79:143–148.
35. Ohtaka M. Stroke-prone SHR (SHRSP) as models for clinical and epidemiological studies on hypertension-related cardiac diseases in humans. *Jpn Circ J* 1980; 44:347–360.
36. Klimas J, Stankovicova T, Kyselovic J, Bacharova L. Prolonged QT interval is associated with blood pressure rather than left ventricular mass in spontaneously hypertensive rats. *Clin Exp Hypert* 2008; 30:475–485.
37. Ohtaka M. Vectorcardiographical and pathological approach to the relationship between cardiac hypertrophy and coronary arteriosclerosis in spontaneously hypertensive rats (SHR). *Jpn Circ J* 1980; 44:283–293.

Reviewers' Summary Evaluations

Referee 1

This comparative longitudinal analysis on cardiac function in normotensive and spontaneously hypertensive rats (SHR) provides a detailed analysis of cardiac function by echocardiography, electrocardiography and left ventricular pressure measurements. The authors demonstrate that echocardiographic indicators of diastolic dysfunction are differentially affected by short-term reductions in afterload and provide a valuable collection of echocardiographic reference values. The study shows that aged SHR can be used as preclinical model to investigate the pathology and pharmacology of diastolic dysfunction in great detail.

Referee 2

This is a longitudinal study on spontaneously hypertensive rats aged 28 to 53 weeks, by echocardiography, electrocardiography, blood pressure measurements, and assessment of collagen deposition, synthesis and degradation. Since this model showed progressive alterations in early filling dynamics associated with preserved systolic function, the authors suggest its role as a relevant 'experimental model' of heart failure with preserved ejection fraction (HF-PEF). This adds on recent literature on the transition from compensated pressure-overload hypertrophy to heart failure in showing that diastolic alterations are evident before evidence of chamber systolic dysfunction, changes in extracellular matrix turnover being key mechanisms in this process.